

Demonstration of zero optical backscattering from single nanoparticles

Steven Person,¹ Manish Jain,¹ Zachary Lapin,^{1,2} Juan Jose Sáenz,³ Gary Wicks,¹ and Lukas Novotny^{1,2}

¹*Institute of Optics, University of Rochester, Rochester, New York 14627, USA*

²*ETH Zürich, Photonics Laboratory, 8093 Zürich, Switzerland*

³*Departamento de Física de la Materia Condensada,*

Instituto “Nicolás Cabrera” and Centro de Investigación en Física de la Materia Condensada (IFIMAC), Universidad Autónoma de Madrid, 28049-Madrid, Spain.

(Dated: September 10, 2018)

We present the first experimental demonstration of zero backscattering from nanoparticles at optical frequencies as originally discussed by Kerker *et. al.* [M. Kerker, D. Wang, and C. Giles, J. Opt. Soc. A **73**, 765 (1983)]. GaAs pillars were fabricated on a fused silica substrate and the spectrum of the backscattered radiation was measured in the wavelength range 600-1000 nm. Suppression of backscattering occurred at ~ 725 nm, agreeing with calculations based on the discrete dipole approximation. Particles with zero backscattering provide new functionality for metamaterials and optical antennas.

PACS numbers: 42.25.Fx, 78.67.Bf, 42.25.Hz

Nanofabrication techniques continue to fuel the search for structures that exhibit unique optical properties. Among these structures are optical antennas, which concentrate and direct light [1], and metamaterials that can mimic optical constants not found in nature [2, 3]. Optical antennas and metamaterials often capitalize on the plasmonic properties of metal nanostructures [4, 5]. Plasmons, however, have large non-radiative losses that restrict practical applications to narrow frequency bands [6], even if active gain media are employed [7]. Recently, alternative approaches using dielectric materials have been proposed for constructing optical antennas [8–11] and metamaterials [12–14].

The optical properties of dielectric nanostructures are strongly influenced by the interaction of electric and magnetic Mie resonances. Thirty years ago, Kerker *et. al.* showed that the backscattered light from spherical scatterers can be completely suppressed if the dielectric and magnetic properties of the scatterers are the same ($\epsilon = \mu$) [15]. A particle with these properties exhibits equal electric (a_n) and magnetic (b_n) multipole coefficients [16] that destructively interfere in the backward propagating direction (first Kerker condition). Until recently, zero backscattering at visible wavelengths has been a theoretical curiosity [17–19] due to the lack of magnetic materials ($\mu \neq 1$) in the optical regime.

Kerker’s condition for zero backscattering can be generalized for spherical particles assuming that the scattered field is sufficiently described by the electric (a_1) and magnetic (b_1) dipole terms of the Mie expansion [20]. In terms of a_1 and b_1 the electric and magnetic polarizabilities are defined as

$$\alpha_e = \frac{3i\epsilon}{2k^3}a_1 \quad \alpha_m = \frac{3i}{2\mu k^3}b_1 \quad (1)$$

respectively, where $k = 2\pi n_m/\lambda$, with n_m being the refractive index of the surrounding medium and λ the vac-

uum wavelength. The two dipoles interfere constructively or destructively depending on their relative phase. In the backward direction the particle’s scattering cross-section is

$$\sigma_b = 4\pi k^4 I_\alpha \left[1 + V_\alpha \cos(\pi - \Delta\phi_\alpha) \right] \quad (2)$$

where $I_\alpha = |\alpha_e/\epsilon|^2 + |\mu\alpha_m|^2$ is the incoherent sum of the two dipoles, $\Delta\phi_\alpha$ is the phase difference between the dipoles, and V_α , given by

$$V_\alpha = \frac{2|\alpha_e/\epsilon||\mu\alpha_m|}{I_\alpha}, \quad (3)$$

controls the backscattering suppression. A minimum in the backscattered field will occur whenever the electric and magnetic dipoles are oscillating in phase ($\Delta\phi_\alpha = 0$). The minimum will be exactly zero if V_α is equal to one.

Note that the elimination of the backscattered field in Eq. (2) is valid even for non-magnetic materials ($\mu = 1$) provided that the dipole approximation holds. This approximation requires dielectric nanoparticles with a large index of refraction ($n \sim 3 - 4$), such as

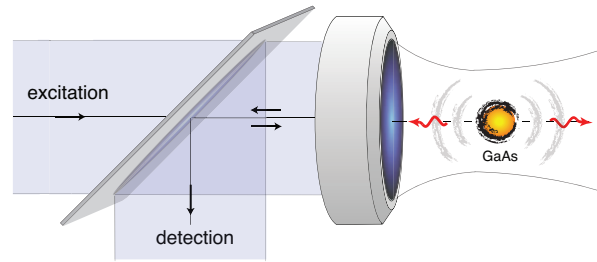


FIG. 1: Illustration of the backscattering measurement. White light is weakly focused on a GaAs particle of radius ~ 90 nm. Backscattered light is separated by a 50/50 beam-splitter and sent to a spectrometer.

silicon and germanium [21, 22]. Recently, the electric and magnetic dipole and quadrupole resonances have been experimentally measured for silicon spheres in the visible [23–25]. The large refractive index of these nanoparticles make them ideally suited for verifying Kerker’s theoretical predictions.

In this letter we experimentally demonstrate the suppression of optical backscattering from dielectric nanoparticles, as predicted by Kerker [15]. A recent experiment has demonstrated suppressed backscattering at microwave frequencies [26], however, a verification at optical wavelengths has not yet been performed. We chose GaAs as a scattering material due to its large index of refraction ($n \sim 3.6$) in the 600 to 1000 nm wavelength range [27]. The experimental arrangement is sketched in Fig. 1: white light is weakly focused on a sample of well separated GaAs nanoparticles and the backscattered light is separated by a beamsplitter and directed on a spectrometer. Fig. 2(a) is a plot of the extinction efficiency ($Q_{\text{ext}} = \sigma_{\text{ext}}/\pi r^2$) for a GaAs sphere of radius $r=90$ nm immersed in a medium of index $n_m = 1.47$. The contributions of the dipole terms (a_1, b_1) and the quadrupole terms (a_2, b_2) of Q_{ext} are shown as separate curves. The curves show that for wavelengths longer than ~ 600 nm the electric and magnetic quadrupole terms can be neglected. The backscattering efficiency ($Q_b = \sigma_b/\pi r^2$) is plotted in Fig. 2(b). A minimum in Q_b is located at ~ 775 nm where the relative phase between the electric and magnetic dipoles crosses zero ($\Delta\phi_\alpha \sim 0$).

To measure backscattering from GaAs nanoparticles embedded in a uniform environment we implemented an epitaxial lift-off technique in conjunction with a water-bonding procedure to attach a high quality GaAs

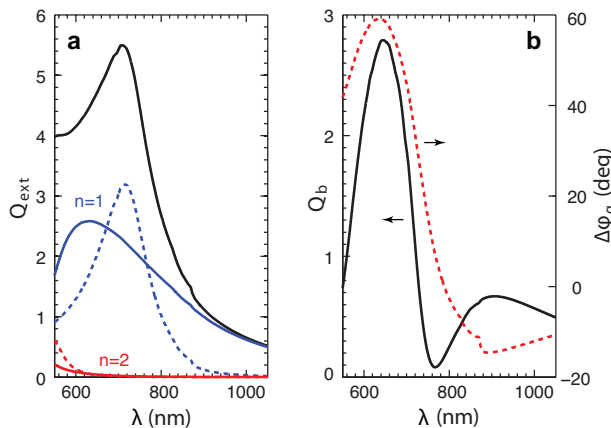


FIG. 2: Mie theory calculations of a 90 nm radius sphere of GaAs embedded in a uniform medium of refractive index $n_m = 1.47$. (a) Electric (solid) and magnetic (dashed) dipole ($n=1$) and quadrupole ($n=2$) contributions to the total extinction efficiency (Q_{ext}). (b) Backscattering efficiency (Q_b) and phase difference ($\Delta\phi_\alpha$) between the electric and magnetic dipoles.

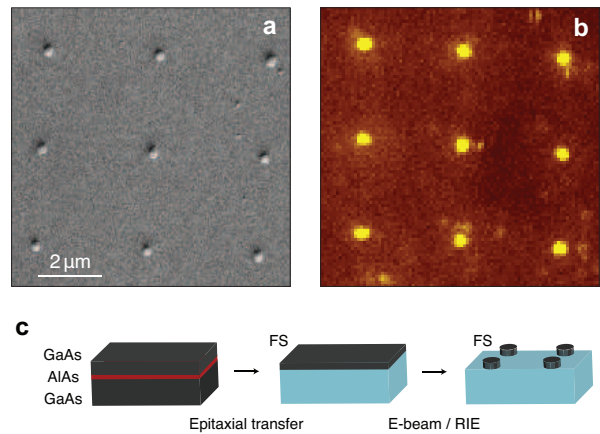


FIG. 3: (a,b) Characterization of the fabricated GaAs nanoparticle sample. (a) SEM image of an array of GaAs pillars of radius $r \sim 90$ nm. (b) Confocal photoluminescence image of the same sample area. Wavelength of excitation laser: $\lambda = 532$ nm. (c) Steps of the sample fabrication process showing the transfer of the GaAs epitaxial layer to a fused silica (FS) substrate and the generation of GaAs pillars with e -beam lithography and reactive-ion etching (RIE).

membrane (grown on a GaAs substrate) to a fused silica substrate [28, 29]. Direct growth of GaAs on fused silica is avoided because it results in a high density of dislocations. Figure 3(b) illustrates the fabrication steps. Using molecular beam epitaxy (MBE), a 40 nm sacrificial layer of AlAs was deposited on a GaAs substrate. On top of the AlAs layer a $1 \mu\text{m}$ film of GaAs was grown. Using the epitaxial lift-off procedure, the $1 \mu\text{m}$ GaAs film was transferred to a fused silica substrate. The transferred GaAs film was initially reduced to a thickness of ~ 150 nm by reactive ion etching (RIE). An array of ~ 175 nm diameter discs was then patterned in a Poly(methyl methacrylate) (PMMA) resist using e -beam lithography. After developing the resist, GaAs pillars were created by RIE. The leftover PMMA was removed with an additional oxygen plasma etch. Fig. 3(a) shows a scanning electron microscope (SEM) image of the fabricated structures. To verify that no residual GaAs remained after etching, a confocal scanning image of the photoluminescence was taken with an excitation laser of $\lambda = 532$ nm. The confocal image in Fig. 3(b) shows strong signal from the GaAs pillars with limited luminescence from the fused silica substrate.

Backscattering measurements were done using a standard inverted microscope with a fiber-coupled tungsten halogen white light source (c.f Fig. 1). To create a uniform environment, and eliminate any back-reflections, index matching oil covered the top of the sample. The sample was broadly illuminated by weakly focusing the white light source through an oil immersion objective. The backscattered light was collected with the same objective and sent to either an avalanche photodiode

(APD) or a spectrometer. A 10 nm bandpass filter was placed in front of the APD and the sample was scanned by a piezo positioning stage to form an image. Spectra of single GaAs pillars were acquired in the wavelength range of 600-1000 nm. The collection volume was limited either by the APD detector area or the spectrometer slit width. This ensured that light from only a single scatterer was detected even though the sample was broadly illuminated.

The recorded spectra and APD images were corrected for source spectrum non-uniformity, transmission losses, and detector efficiencies. A baseline spectrum [$I_{\text{mirror}}(\lambda)$] was recorded by replacing the sample with a mirror. Additionally, the background spectrum [$I_{\text{bkg}}(\lambda)$] measured on the fused silica substrate away from the GaAs pillars was subtracted. This background resulted from a slight refractive index mismatch between substrate and index-matching oil. The final backscattering efficiency is calculated as

$$Q_b(\lambda) = \beta \frac{I_{\text{meas}}(\lambda) - I_{\text{bkg}}(\lambda)}{I_{\text{mirror}}(\lambda)}, \quad (4)$$

where I_{meas} is the recorded spectrum. The pre-factor β is a calibration scaling factor.

Figure 4 shows the resulting backscattering efficiency recorded for a single GaAs pillar. The spectrum has a pronounced dip at ~ 725 nm where the backscattered field is suppressed due to the interference between the electric and magnetic dipole components. Though the suppressed backscattered field is obvious, there are two notable differences in the spectral shape when comparing to the Mie theory of Fig. 2. First, the scattering amplitude below ~ 700 nm is suppressed and,

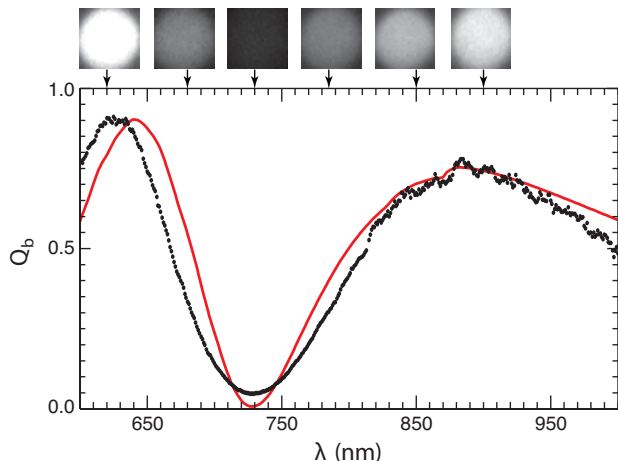


FIG. 4: Backscattering spectrum from a single GaAs pillar. The black dotted curve is the measured spectrum and the red curve is the theoretical spectrum calculated using the discrete dipole approximation. The series of images above the graph are backscattering images of a GaAs pillar recorded with 10 nm bandpass filters at various center wavelengths.

second, the location of the minimum is blue shifted. Both of the differences are attributed to the fact that the structure is a pillar rather than a sphere. Compared to a sphere of the same volume, a pillar with an aspect ratio (height/diameter) below one will have the location of the minimum blue shifted and the scattering peak to the left of the minimum suppressed (See Supplementary Material [30]). The solid curve in Fig. 4 is a simulation of the backscattered field of a GaAs pillar calculated using the discrete dipole approximation [31]. The simulated structure has a height of 137 nm and a diameter of 165 nm, which is within 10% of the initial design parameters. The sequence of images above Fig. 4 are backscattering images with bandwidth of 10 nm and center wavelengths indicated by the arrows. At the location of the spectral minimum the image of the scatterer fades into the background.

In conclusion, we have shown the first experimental verification of Kerker's theoretical prediction of zero backscattering in the *optical* wavelength range. Using pillars, rather than spheres, slight shifts of the wavelength of minimum backscattering can be observed. This shift as well as the reshaping of the spectrum are reproduced with calculations based on the discrete dipole approximation. Understanding and verifying the response of single dielectric nanoparticles is crucial in any bottom-up nanofabrication technique. The remarkable properties of these particles, with zero backscattering but significant light dispersion in forward direction, suggest intriguing technological applications, for example as light diffusing elements in solar cells. Using similar GaAs structures, experiments involving arrays of scatterers [32] or dielectric antennas manipulating magnetic dipoles [33, 34] are possible.

This work was funded by the U.S. Department of Energy (Grant No. DE-FG02-01ER15204).

-
- [1] P. Bharadwaj, B. Deutsch, and L. Novotny, *Adv. Opt. Phot.* **1**, 438 (2009).
 - [2] V. M. Shalaev, *Nature Photon.* **1**, 41 (2007).
 - [3] C. M. Soukoulis and M. Wegener, *Nature Photon.* **5**, 523 (2011).
 - [4] J. A. Schuller, E. Barnard, W. Cai, Y. C. Jun, J. White, and M. L. Brongersma, *Nature Mat.* **9**, 193 (2010).
 - [5] S. Kawata, Y. Inouye, and P. Verma, *Nature Photon.* **3**, 388 (2009).
 - [6] M. Stockman, *Phys. Rev. Lett.* **98**, 177404 (2007).
 - [7] O. Hess, J. B. Pendry, S. A. Maier, R. F. Oulton, J. M. Hamm, and K. L. Tsakmakidis, *Nature Mat.* **11**, 573 (2012).
 - [8] J. A. Schuller and M. L. Brongersma, *Opt. Express* **17**, 24084 (2009).
 - [9] B. Rolly, B. Stout, and N. Bonod, *Opt. Express* **20**, 20376 (2012).

- [10] W. Liu, A. E. Miroshnichenko, D. N. Neshev, and Y. S. Kivshar, *ACS Nano* **6**, 5489 (2012).
- [11] A. Devilez, B. Stout, and N. Bonod, *ACS Nano* **4**, 3390 (2010).
- [12] J. A. Schuller, R. Zia, T. Taubner, and M. L. Brongersma, *Phys. Rev. Lett.* **99**, 107401 (2007).
- [13] Q. Zhao, J. Zhou, F. Zhang, and D. Lippens, *Mater. Today* **12**, 60 (2009).
- [14] L. Jylha, I. Kolmakov, S. Maslovski, and S. Tretyakov, *J. Appl. Phys.* **99**, 043102 (2006).
- [15] M. Kerker, D. Wang, and C. Giles, *J. Opt. Soc. Am.* **73**, 765 (1983).
- [16] C. F. Bohren and D. R. Huffman, *Absorption and Scattering of Light by Small Particles* (Wiley, New York, 1983).
- [17] B. García-Cámara, F. Moreno, F. González, J. M. Saiz, and G. Videen, *J. Opt. Soc. Am. A* **25**, 327 (2008).
- [18] B. García-Cámara, R. Alcaraz de la Osa, J. M. Saiz, F. González, and F. Moreno, *Opt. Lett.* **36**, 728 (2011).
- [19] B. García-Cámara, J. María Saiz, F. González, and F. Moreno, *Optics Comm.* **283**, 490 (2010).
- [20] M. Nieto-Vesperinas, R. Gómez-Medina, and J. J. Sáenz, *J. Opt. Soc. Am. A* **28**, 54 (2011).
- [21] R. Gómez-Medina, B. García-Cámara, I. Suárez-Lacalle, F. González, F. Moreno, M. Nieto-Vesperinas, and J. J. Sáenz, *J. Nanophotonics* **5**, 053512 (2011).
- [22] A. García-Etxarri, R. Gómez-Medina, L. S. Froufe-Pérez, C. López, L. Chantada, F. Scheffold, J. Aizpurua, M. Nieto-Vesperinas, and J. J. Sáenz, *Opt. Express* **19**, 4815 (2011).
- [23] A. I. Kuznetsov, A. E. Miroshnichenko, Y. H. Fu, J. Zhang, and B. Luk'yanchuk, *Sci. Rep.* **2**, 492 (2012).
- [24] A. B. Evlyukhin, S. M. Novikov, U. Zywietz, R. L. Eriksen, C. Reinhardt, S. I. Bozhevolnyi, and B. N. Chichkov, *Nano Lett.* **12**, 3749 (2012).
- [25] M. S. Wheeler, J. S. Aitchison, J. I. L. Chen, G. A. Ozin, and M. Mojahedi, *Phys. Rev. B* **79**, 073103 (2009).
- [26] J. Geffrin, B. García-Cámara, R. Gómez-Medina, P. Albella, L. Froufe-Pérez, C. Eyraud, A. Litman, R. Vaillon, F. González, M. Nieto-Vesperinas, et al., *Nature Commun.* **3**, 1171 (2012).
- [27] E. D. Palik, *Handbook of Optical Constants of Solids* (Elsevier, San Diego, 1998).
- [28] E. Yablonovitch, T. Gmitter, J. Harbison, and R. Bhat, *Appl. Phys. Lett.* **51**, 2222 (1987).
- [29] P. Demeester, I. Pollentier, P. Dedobbelaere, C. Brys, and P. Vandaele, *Semicond. Sci. Technol.* **8**, 1124 (1993).
- [30] *See supplemental material at [url will be inserted by publisher] for scattering properties of gaas cylinders.*
- [31] B. T. Draine and P. J. Flatau, *J. Opt. Soc. Am. A* **11**, 1491 (1994).
- [32] A. B. Evlyukhin, C. Reinhardt, A. Seidel, B. S. Luk'yanchuk, and B. N. Chichkov, *Phys. Rev. B* **82**, 045404 (2010).
- [33] M. K. Schmidt, R. Esteban, J. J. Sáenz, I. Suárez-Lacalle, S. Mackowski, and J. Aizpurua, *Opt. Express* **20**, 13636 (2012).
- [34] B. Rolly, B. Bebey, S. Bidault, B. Stout, and N. Bonod, *Phys. Rev. B* **85**, 245432 (2012).